Immunization with *Mycobacterium tuberculosis* antigens encapsulated in phosphatidylserine liposomes improves protection afforded by BCG

Gil R. Diogo[1#]; Peter Hart[1#;] Alastair Copland[1#]; Mi-Young Kim[1], Andy C. Tran[1]; Noemi Poerio[3], Mahavir Singh[2]; Matthew J. Paul[1], Maurizio Fraziano[3] and Rajko Reljic[1*]

[1] St George's University of London, SW17 0RE, United Kingdom

[2] Lionex, Braunschweig, 38126, Germany

[3] University of Rome Tor Vergata, Rome, 00133 Roma, Italy

# These authors contributed equally to this work

* Corresponding author: Dr Rajko Reljic

St George's University of London, SW17 0RE, United Kingdom

E-mail: rreljic@sgul.ac.uk; Tel: +0208-725 0554

Key words: liposomes, tuberculosis, vaccine, BCG, immunity

Abstract

Liposomes have been long considered as a vaccine delivery system but this technology remains to be fully utilised. Here, we describe a novel liposome-based subunit vaccine formulation for tuberculosis (TB) based on phosphatidylserine encapsulating two prominent TB antigens, Ag85B and ESAT-6. We show that the resulting liposomes (Lipo-AE) are stable upon storage and can be readily taken up by antigen presenting cells and that their antigenic cargo is delivered and processed within endosomal cell compartments. The Lipo-AE vaccine formulation combined with the PolyIC adjuvant induced a mixed Th1/Th17-Th2 immune response to Ag85B but only a weak response to ESAT-6. An immunisation regimen based on systemic delivery followed by mucosal boost with Lipo-AE resulted in the accumulation of resident memory T cells in the lungs. Most importantly though, when Lipo-AE vaccine candidate was administered to BCG-immunised mice subsequently challenged with low dose aerosol *Mycobacterium tuberculosis*, we observed a significant reduction of the bacterial load in the lungs and spleen compared to BCG alone. We therefore conclude that the immunization with mycobacterial antigens delivered by phosphatidylserine based liposomes in combination with Poly:IC adjuvant may represent a novel BCG boosting vaccination strategy.

Introduction

Despite the availability of a vaccine and drug regimens, tuberculosis (TB) remains a major health burden globally. In 2016, there were approximately 1.3 million deaths from TB among HIV-negative and 374,000 among HIV-positive individuals, making it the 9th cause of death worldwide and the number one due to a single infectious agent (Churchyard et al., 2017).

The current vaccine, Bacille Calmette Guérin (BCG), was first administered nearly 100 years ago and is still extensively used today. BCG was first used in children in 1921 and is now given to more than 120 million people worldwide every year, with 4 billion people already immunised (Ottenhoff and Kaufmann, 2012). It is effective at preventing severe forms of TB in children but provides varying levels of protection against pulmonary TB in adults. Revaccination with BCG has not been shown to be advantageous (Rodrigues et al., 2005;Roth et al., 2010) and is not recommended by the WHO. Coupled with the emergence of multi-drug resistant tuberculosis (MDR-TB) with unsatisfactory treatment rates, it is clear that a more effective TB vaccine is a major healthcare priority.

Although there are several vaccine candidates at various stages of clinical trials and many more at preclinical stage of research and development, it is important to continuously feed the TB vaccine pipeline with both live and subunit vaccines. This is because it may well be that more than a single vaccination strategy will be needed to protect different human populations against TB (eg. different age groups, HIV status, geographical location etc). For example, a replacement BCG vaccine is likely to be another live attenuated organism (recombinant BCG or attenuated *Mtb*) in order to protect young children from severe primary TB infection but a subunit vaccine may be

preferable in HIV-positive population due to the host's immunocompromised state. Likewise, it may be preferable to boost BCG with a subunit rather than another attenuated vaccine to avoid excessive delayed hypersensitivity reactions (Koch's phenomenon). Recombinant protein subunit vaccines are inherently safer but are often weakly immunogenic and require adjuvants and/or specialised delivery systems to induce protective immunity.

One such delivery system is liposomes, which were identified as a potential drug delivery platform in the 1970s. However, the discovery that liposomes preferentially target tissue macrophages (Ellens et al., 1981) highlighted their potential also as a vaccine delivery system (Gregoriadis, 1990;Wassef et al., 1994). Subsequently, they have been used in the context of both bacterial (Lachman et al., 1996;Fulton et al., 1998) and viral infections (Ambrosch et al., 1997) and even in cancer immunotherapies (Kwak et al., 1998). An attractive characteristic of the liposomal delivery platforms is that they can shelter antigens from degradation, promote phagocytosis by antigen-presenting cells (APCs) (Wassef et al., 1994) and induce phagosome-cytosol cross-presentation pathway of antigenic peptides on MHC Class I molecules (Kovacsovics-Bankowski and Rock, 1995;Sigal et al., 1999).

The apoptotic body-like liposomes (ABLs, Fig.1A) used in the present study are prepared from phosphatidylserine (PS), rendering them similar to apoptotic bodies. PS is hydrophilic and appears on the surface of early apoptotic cells (Fadok et al., 1992); this 'flags up' the dying cells as a target for APCs such as macrophages and dendritic cells (DC) (Tanaka and Schroit, 1983;Schlegel and Williamson, 2001). It is thought that this phenomenon can augment the presentation of the antigens by APCs, leading to improved T cell responses (Ichihashi et al., 2013). As a cell initiates apoptosis, the PS normally situated on the inner face of the lipid bilayer of the cell

membrane is exposed (Fadok et al., 1992). PS is implicated in the detection of apoptotic cells by its interaction with Tim4 and Tim1 on APC, which facilitates phagocytosis (Miyanishi et al., 2007).

We therefore hypothesized that the PS associated antigens will similarly be taken up by professional APCs resulting in their cross-presentation and amplification of the immune response. Here, we present the evidence for the utility of this vaccine delivery system by demonstration that liposomally encapsulated *Mtb* antigens can enhance BCG-afforded protection against tuberculosis infection in mice.

Materials and methods

Generation of PS liposomes

Briefly, the inner monolayer lipid was prepared by suspending phosphatidylserine (PS, Avanti Polar Lipids) in 1 ml of anhydrous dodecane at the concentration of 0.2 mg/ml, sonication for 30 minutes and overnight incubation. The following day, 10 µg of Ag85B or ESAT-6 (Lionex Diagnostics and Therapeutics), or bovine serum albumin conjugated to Alexafluor488 (AF488-BSA), Alexafluor647 (AF647) (Molecular Probes) or ovalbumin conjugated to BODIPY® FL [500 µg/ml] (DQ-OVA), were added to inner monolayer lipid suspension and sonicated until a homogeneous solution was obtained. The inner monolayer lipid for empty control liposomes was prepared using the same buffer used to suspend the respective antigen. The outer lipid monolayer was prepared by suspending PS in 99:1 dodecane: silicone solution to get a lipid concentration of 0.05 mg/ml. Thereafter, 2 ml of outer monolayer lipid suspension was added to 3 ml of 0.9% NaCl solution. Finally, the inner monolayer lipid suspension was

added to 2 ml lipid phase and the sample was centrifuged at 120 x g for 10 minutes. After the centrifugation, liposomes were collected in the aqueous phase using a 5 ml syringe with a 16-gauge stainless steel needle. Liposomes were quantified and characterized in terms of dimensions as described(Greco et al., 2012). To determine antigen recovery following encapsulation, liposomes were dialysed against a 100 kDa membrane (Float-A-Lyzer® G2, Spectrum Labs), according to manufacturer's instructions. Encapsulated antigen was then quantified by CBQCA Protein Quantitation Kit (C-6667 Molecular Probes) according to manufacturer's instructions by fluorimetric analysis (Thermofisher VARIOSKAN LUX). The schematic representation of liposomes with encapsulated antigen is shown in Fig.1A. For the final vaccine formulation, equal numbers of Ag85B and ESAT-6 encapsulating liposomes were combined to generate the Lipo-AE vaccine candidate.

Generation of human DC

Human blood monocytes from healthy volunteers were separated from peripheral blood mononuclear cells (PBMCs), by using anti-CD14 monoclonal antibodies conjugated to magnetic microbeads (Miltenyi Biotec), according to manufacturer's instructions. To obtain immature dendritic cells (iDc), cells were suspended in complete medium (RPMI 1640 supplemented with 10% fetal bovine serum, 2 mM L-Glutamine and 5 µg/ml Gentamicin) and incubated for 5 days in 24-well plates at the concentration of $5x10^5$ cells/well in the presence of 20 ng/mL GM-CSF (Sigma-Aldrich) and 20 ng/mL IL-4 (Miltenyi Biotec). To obtain mature dendritic cells (mDC), iDCs were further stimulated for 18 hours with 100 ng/ml lipopolysaccharides (Sigma-Aldrich).

Flow cytometry analysis of stability and antigen delivery by PS liposomes

The stability of PS liposomes loaded with AF488-BSA was assessed in terms of fluorescence intensity immediately and at 30 days after their preparation by flow cytometry analysis. Antigen internalization was analysed after incubation of immature (iDC) or mature DC (mDC) with PS liposomes loaded with bovine serum albumin conjugated to Alexafluor647 (BSA-AF647) (Molecular Probes), at the ratio liposome : cell of 5:1, for 1 hour at 37 °C. Antigen processing was evaluated in iDC after exposure to ovalbumin conjugated to BODIPY® FL (DQ-OVA), a self-quenched conjugate that exhibits bright green fluorescence upon proteolytic processing and red fluorescence upon accumulation of proteolysed fragments in endosomal compartments. The analyses were performed by a FACSCalibur flow cytometer (Becton Dickinson).

Confocal microscopy analysis of antigen processing in dendritic cells

Briefly, iDC were stained with the nucleic acid stain Hoechst (Molecular Probes) and the acidophilic dye Lysotraker Red (Molecular Probes) for 15 minutes at 37°C. Thereafter, cells were washed with PBS, and exposed to PS liposomes loaded with AF488-BSA at the ratio 5:1 (liposome:cell) for 90 minutes at 37 °C. The analysis was performed by a confocal laser scanning microscope IX 81 and OLYMPUS FV1000 operating system.

Animals

All animals were used with approval from St George's University of London Ethics Committee under an approved UK Home Office animal project licence and used in accordance with the Animals (Scientific Procedures) Act 1986. 8-10 week old female C57BL/6 mice were used for this study and were obtained from Charles River, UK. Animal work was conducted at St. George's University of London Biological Research Facility in accordance with local guidelines, including approval from the St George's University of London Research Ethics Committee and national legislation, the Animals in Scientific Procedures Act, 1986. All procedures were performed under the approved UK Home Office animal project licence.

Recombinant proteins

Ag85B and ESAT-6 antigens of *Mtb* were produced in *E. coli* by Lionex company (Braunschweig, Germany) using the standard cloning techniques and the IPTG-inducible expression vector pLEXWO481. Recombinant proteins were isolated from inclusion bodies after denaturation in 8 M urea using metal chelate chromatography (Ni-NTA Superflow, Qiagen) and subsequent refolding by dialysis. Purity was assessed by SDS-PAGE (>97% purity) and identity confirmed by Western blots specific for antigens. Endotoxin content was measured by LAL assay and determined to be <5 I.U. / mg.

Immunisations

Mice were first immunised subcutaneously at the base of the tail with 5 x 10^5 CFU BCG Pasteur in 0.1 ml or a matched volume of phosphate saline solution (Sigma) as

a control. 10 weeks later, mice received 0.1 ml of Lipo-AE formulation (containing approximately 10^6 liposomes, 1 μg of Ag85B and 0.2 μg ESAT-6) also by s.c. injection at the base of the tail and then 3 weeks later a further intranasal inoculation of 0.05 ml of the same formulation, while under light anaesthesia. All Lipo-AE immunisations included 20 μg/per dose of poly(I:C) as the adjuvant. Further details of the dosing regimen are given in the corresponding figure legends.

Low-dose aerosol Mtb infection and bacterial enumeration

Mice were infected 4 weeks after the final immunisation by aerosol with *Mtb* (H37Rv strain) at a low dose of approximately 200 bacilli per animal. The dose was delivered by nose only exposure using the Biaera aerosol generator controlled by the AeroMP software (Biaera Technologies) and housed in a dedicated Containment Level 3 (CL3) laboratory at Biological Research facilities at St George's. Mice were left infected for four weeks before culling and bacterial enumeration in the lungs and spleens. The organs were homogenised in 3 ml of 0.1 % Triton x-100 using the Precellys equipment. Serial dilutions of the homogenate were prepared and plated on Middlebrook 7H11 plates supplemented by OADC (Becton Dickinson) and bacterial colonies counted three weeks later. The pathogenic *Mtb in vitro* work was performed in the CL3 TB suite at the Institute for Infection and Immunity at St George's.

Mucosal antibody responses

IgG and IgA in bronchoalveolar lavage (BAL) specific for antigens was measured by ELISA. Antigens (Ag85B or ESAT-6, Lionex) at 2 μg/ml were used to coat the wells of

an ELISA plate. After washing with PBS 0.05% v/v Tween-20 and blocking with PBS 1% w/v BSA, 0.05% v/v Tween-20, samples were added in 3-fold dilutions. Specific IgG and IgA were detected with alkaline phosphatase conjugated anti-mouse IgG (Jackson Immunoresearch) and anti-mouse IgA (Sigma), respectively, and the substrate SigmaFast p-nitrophenyl phosphate (Sigma). Triplicate assays were read at 450 nm on a Tecan200 plate reader and data plotted as relative antibody titres as described in Hart et al 2017 (Hart et al., 2018).

T cell proliferation, cytokine production and lung Trm

T cell proliferation was assessed by measuring the incorporation of radio-labelled thymidine [^{3}H] after stimulation of splenocytes with recall antigens. Erythrocyte-depleted splenocytes were seeded at 1.5 x 10^{5}/well in complete RPMI 1640 medium supplemented with 10 % FBS and stimulated with 5 μg/ml antigen or 1 μg.ml ConA as the positive control. After 48 h incubation, 1 μiCi of ^{3}H-thymidine (PerkinElmer, Wallac, UK) was added before a further 24h incubation. Cells were harvested with the Harvester 96 (TomTec Life Sciences, Hamdem, USA) onto Printed Filtermat paper (PerkinElmer) prior to the addition of melted wax (MeltiLex TM A. PerkinElmer) onto each scintillation sheet. Radioactive counts per minute (cpm) were measured using the 1450 Microbeta Plus-Liquid Scintillation Counter (PerkinElmer).

For phenotypic analysis of proliferating T cells, splenocytes were stimulated with 5 μg/mL Ag85B or 1 μg/mL α-CD3 (Biolegend) for 5 days, followed by surface staining with CD4-PerCP/Cy5.5, CD8-Brilliant Violet 510, CD44-FITC, CD62L-PE and CD90.2-Brilliant Violet 421 — all from Biolegend. Cells were then fixed and permeabilised

using the eBioscience Foxp3 / Transcription Factor Staining Buffer Set and stained with Ki67-APC. Example of gating strategy is shown in Supplemental Fig.S1.

Culture supernatant cytokine levels were measured using the mouse LegendPlexTM kit (Biolegend) according to the manufacturer's instructions. Samples were acquired on a BD FACSCalibur, and data analysed using the proprietary data analysis software (Biolegend).

For detection of lung resident memory T cells (Trm), lungs were perfused of blood by flushing PBS through the right ventricle. Tissue was then dissected into 1 mm pieces using a scalpel, followed by digestion in 1 mg/mL collagenase and 0.5 mg/mL DNase I (Roche). Cells were then passed through a 70 µm strainer (Becton Dickinson), contaminating erythrocytes were lysed, and mononuclear cells were stained for CD3-APC, CD4-PerCP/Cy5.5, CD8-Brilliant Violet 510, CD44-FITC, CD62L-PE, CD69-PE/Cy7 and CD103-Brilliant Violet 421 — all from Biolegend. Gating strategy as in (Hart et al., 2018).

Sample size, data presentation and statistical analysis

For animal experiments, sample size calculations for *Mtb* challenge studies were based on anticipated magnitude of vaccine effect as 1 Log_{10} reduction of CFU, the intragroup variability of 0.5 Log_{10} and a confidence level of 95%. This necessitated 6 mice per group but due to protracted nature of experiments 7 were used per group. For immunological evaluation 3 mice per group were used and data expressed as arithmetic means +/- standard error. Two in vivo experiments were performed with similar outcomes with the dataset from one experiment shown in full in Figures 3-7,

and only *Mtb* challenge data from the second experiment shown in the Supplemental information. For all experiments based on multiple test groups, One-way ANOVA was performed followed by Dunnett's multiple comparison test. Further details of statistical analyses are described in the relevant figure legends. All analysis was performed using FlowJo v10, Microsoft Excel 2010 and GraphPad Prism 7.

Results

Biophysical characterization and uptake analysis of PS liposomes

Stability is an important issue to be addressed during the generation of novel liposome based vaccine formulations in order to ensure efficient antigen delivery (Nisini et al., 2018). This issue has been addressed by monitoring the kinetics of the encapsulation of fluorescently labelled AF488-BSA, used as a model antigen. The analysis performed by flow cytometry and illustrated in Fig.1B shows that liposomes with encapsulated AF488-BSA remain stably fluorescent up to 30 days upon generation and storage at 4^{o} C. Then, we encapsulated PS liposomes with mycobacterial antigens (Ag85B and ESAT-6) and further tested the physical properties of the novel liposome formulation in terms of size distribution by a Malverin Zetasizer. Results shown in Fig.1C indicate that the formulation was largely homogenous with an average size of the liposomes approximately 240nm.

An antigen delivery system should ideally target APC and promote uptake and processing in dendritic cells (DC). Thus, we preliminarily determined whether PS liposome formulation, encapsulated with AF647-BSA, were efficiently internalized by

immature and mature human DC. In order to avoid the contribution of free antigen, liposome formulations were dialyzed against a 100 kDa membrane to remove non-encapsulated antigen. Fig. 2A shows that the majority of cells became fluorescent after exposure to the liposome formulation, suggesting that most of the cells have taken up the antigen. Moreover, in order to establish whether the antigen was efficiently processed by APC, iDC were exposed to PS liposomes loaded with AF488 BSA and analysed by confocal microscopy after staining with the acidofilic dye lysotraker red. Results shown in Fig. 2B show co-localization of liposomal AF488-BSA with acid compartments. Finally, as acidification of endosomal compartments is a prerequisite for protease activation and the final antigen degradation, we encapsulated PS liposomes with DQ-OVA, which is a fluorogenic substrate for proteases, and monitored fluorescence emission following liposome internalization in iDC. Fig. 2C shows 75% of cells exhibiting green fluorescence, as a consequence of proteolytic processing of the protein, and about 23% of cells displaying green/red double fluorescence, indicating endosomal accumulation of the processed antigen. Altogether, these results show that PS/PS liposomes may efficiently deliver the antigen cargo to DC and favour subsequent antigen processing.

Lipo-AE enhanced BCG mediated protection against Mtb

In our *Mtb* infection experiment, BCG afforded approximately 8-fold reduction in the lung and spleen bacterial load (Fig.3), at four weeks after the aerosol challenge. Boosting BCG with Lipo-AE imparted additional statistically significant reduction of the bacterial load in both organs sets. The *Mtb* challenge experiment was performed twice and in both instances the Lipo-AE vaccine candidate conferred additional statistically

significant protection over BCG alone, though in one of the experiments the nonimmunized animals group showed greater than expected intragroup variability (Supplemental Fig.S2).

Lipo-AE induced mucosal antibodies and T resident memory cells (Trm) in lungs

To measure mucosal responses induced by the vaccine, antibody levels post-immunisation were assessed in bronchoalveolar lavage (BAL). BAL collected three weeks after final immunisation from animals that received Lipo-AE showed similar levels of IgG but higher levels of IgA specific to Ag85B (Fig.4A), compared to BCG immunisation alone. No detectable anti-ESAT-6 antibodies were present in either group (not shown).

Upon observing mucosal antibody responses induced by Lipo-AE, we investigated for evidence of cellular immunity. We were particularly interested if there was evidence of T cell resident memory (Trm) in the lungs and used flow cytometry to quantify these cells in the lung homogenates. Prior to harvest, the lungs were perfused to reduce blood contamination. The harvested lungs were then treated and mechanically disrupted to isolate the cells, which were stained for Trm phenotype (Fig.4B). The top and bottom panels represent CD4 and CD8 compartments, respectively. As depicted in the flow plots the total numbers of Trm as defined by the phenotype CD44 ^{high} / CD62L ^{low} were very low for the BCG immunised animals, and this was true for both the CD4 and CD8 compartments. In stark contrast, there was a significant increase in Trm populations in the Lipo-AE group for both T cell compartments, increasing from 2.04 in the BCG group to 13.22 in the Lipo-AE groups for CD4+ and from 1.50 to 8.16 for CD8+ T cells, respectively (Fig.4B). Naïve animals showed only background levels

of Trm. Although our analysis was restricted to total and not antigen-specific Trm in the lungs, together with the evidence of specific antibodies to Ag85B, it indicates the presence of a mucosal immune response in the lungs of immunised animals.

Splenic T cell proliferation and polyfunctional T cells

We then tested splenocyte proliferation in response to recall antigens as measured by incorporation of radiolabelled thymidine. As shown in Fig.5A, splenocytes from Lipo-AE immunised animals proliferated robustly in response to Ag85B, with a stimulation index of 22, but only modest level of proliferation was observed for ESAT-6, with a stimulation index of 4. Cells from the PBS and BCG groups did not proliferate in response to any of the stimuli. Since liposomes are thought to enhance cross priming and elicit CD8+ T cell responses, T cell proliferation in the CD8+ compartment was additionally investigated by the measurement of Ki67+ cells. Stimulation with Ag85B but not ESAT-6 induced high levels of proliferation in the CD8+ T cell population with most of the proliferating cells being of the $CD62L^{low}$/ $CD44^{High}$ phenotype (Fig.5B). Furthermore, since Lipo-AE induced T cell proliferation (Fig.5A), we speculated that T cell-associated cytokines were also being elicited. To test this, splenocyte culture supernatants were analysed with a beads-based multiplex immunoassay. The analytes tested were IFN-y (Fig.5C), IL-10 (5D), IL-17 (5E) and IL-4 (5F). Stimulation with Ag85B as a recall antigen induced high levels of all cytokines, reflecting a mixed T cell response with the production of Th1 (IFN-y), Th2 (IL-4) and a Treg cytokines (IL-10 and IL-17), with the latter characteristic of Th17 responses. BCG vaccination resulted in minimal cytokine production in these assays.

Splenocytes from Lipo-AE immunised animals displayed low level ESAT-6 responses (not shown) but stimulation with Ag85B resulted in a significant number of cytokine producing CD4+ (1.77%) and CD8+ (0.45%) T cells (Fig.6A,F). In the CD4+ T cell compartment, 1.63% of those cells produced IFN-γ, 1.17% IL-2 and 1.76% TNF-α (Fig.6B). Lipo-AE also induced the highest number of polyfunctional T cells producing three or more of the measured cytokines simultaneously with 1.13% of cells in this category (Fig.6C). A large portion of these cells (1.13%) were triple producers, producing INF-γ, IL-2 and TNF-α simultaneously, with a further population (0.51%) double producers of IFN-γ and TNF-α (Fig.6D). Of the cytokine producing cells, most were triple producers (64%) with 31% producing two cytokines and 5% producing only one of the measured cytokines (Fig.6E).

A similar picture was observed in the CD8+ T cell compartment, where Lipo-AE group splenocytes had the highest number of cytokine producing cells, with 0.11% producing IFN-γ and 0.32% producing IL-17A. The highest number of polyfunctional cells producing 3 or more cytokines simultaneously was also found in the Lipo-AE group (0.036%).

Stimulation with Ag85B resulted in 0.04% of CD8+ T cells producing IFN-γ, IL-2 and IL-17A, with high levels of single cytokine producing cells for IFN-γ, 0.12%, and IL-17A, 0.30%. Of the cytokine producing cells the majority were single producers (92%) with a small proportion of triple producers (8%).

Discussion

Liposomes have been tested in the context of systemic immunizations but also as oral vaccine vehicles (Jackson et al., 1990;Michalek et al., 1992). Despite their relative

instability, liposomes were shown to be robust enough to survive oral delivery to the intestinal lumen and enhance the antigen presentation (Elson et al., 1996). Indeed, our own stability experiments showed that the liposomes used in this study are stable for at least 30 days. Subsequent Zetasizer analysis also demonstrated that the formulation was still homogeneous and the size of the liposomes remained unchanged at approximately 200 nm.

The mucosal delivery of liposomes *in vivo* has been tested extensively through the oral route (Childers et al., 1987;Jackson et al., 1990) and also through the intranasal route (Romero and Morilla, 2011). A comparison between the two routes in terms of ability to induce long term local immune responses seemed to favour the intranasal route (Elson et al., 1996). Here we demonstrate the ability of a novel liposome formulation to protect against *Mtb* infection when delivered first subcutaneously and then intranasally. This vaccine strategy was explored as a heterologous immunisation approach on a BCG background. In human population, boosting BCG would make use of the large number of already immunised individuals whilst taking advantage of protective properties of BCG against severe forms of childhood TB.

Immunisation of mice with BCG reduced the burden of infection significantly in the lungs and spleens in comparison to unvaccinated animals in a low dose aerosol challenge model. This protection afforded by BCG was further increased by boosting with Lipo-AE and this added protection was found to be statistically significant in both the lungs and spleens. Upon observing enhancement of protection conferred by Lipo-AE the immunological profile induced by the vaccine was studied. Other pre-clinical studies demonstrated that liposomes promoted antibody and cell mediated immunity to a wide range of bacterial, protozoan and viral antigens as well as tumour cell antigens, venoms and allergens and even live or attenuated microbial vaccines

(Gregoriadis, 1990). With regards to cellular immunity, we observed that stimulation of splenocytes from vaccinated animals with a recall antigen induced high levels of IFN-y. IgG and IgA specific to Ag85B was also detected by ELISA in BAL indicating the vaccine had also successfully primed the B cells in the mucosa.

With the view of elucidating further what immune mechanisms could be behind the observed protection we further investigated the cellular profiles induced. A cell proliferation assay revealed that splenocytes isolated from Lipo-AE vaccinated animals in culture proliferated in response to Ag85B and to a lesser extent to ESAT-6. These cells produced high amounts of IFN-y in response to Ag85B stimulation. IFN-y is considered essential for resistance to tuberculosis infection (Flynn et al., 1993;Reljic, 2007). However, despite IFN-y being required for protection a number of studies have suggested that other mechanisms may also be needed for protection (Gallegos et al., 2011) and the magnitude of IFN-y response alone is not a reliable correlate of protection (Mittrucker et al., 2007;Sakai et al., 2016).

Splenocytes were also found to produce IL-10, which has an ambiguous role in TB, with some reports showing that it is undesirable (Redford et al., 2011) while other suggesting that it can convert human DCs into macrophage like cells that have increased antibacterial activity against *Mtb* (Fortsch et al., 2000). Intriguingly, high levels of IL-17A were also detected in response to Ag85B and to a lesser extent to ESAT-6 in splenocyte cultures from Lipo-AE vaccinate animals. Whilst the role of IL-17 in *Mtb* infection is not clearly defined it has been reported that its induction after vaccination could be beneficial. Thus, Khader et al, hypothesized that IL-17 producing CD4+ T cells occupy the lung after infection and elicit the production of chemokines that attract IFN-y secreting CD4+ T cells resulting in better control of infection (Khader et al., 2007).

Thus, the cytokine profile characterised by high IFN-y and IL-17A with low levels of IL-10 observed here could be the key to enhanced protection. IL-10 produced by vaccine-induced Tregs could limit collateral damage within the lung. It was suggested that granulomas depended on a balance of inflammatory and anti-inflammatory cytokines in order to effectively control bacteria (Wigginton and Kirschner, 2001). This concept was validated in the Rhesus macaque model, where sterile granulomas were associated with a balance of IFN-y/IL-17A and IL-10 in contrast to the non-sterile granulomas that featured a predominantly inflammatory response lacking IL-10 (Gideon et al., 2015). Finally, evidence from *T. gondii* model of infection has shown that multifunctional IL-10-producing Th1 cells retain their ability to activate intracellular killing mechanisms in macrophages, and in fact are superior to conventional IL-10 negative Th1 cells at inducing macrophage nitrite (NO) production (Jankovic and Trinchieri, 2007). Given that we observed modest IL-10 and even lower IL-4 production alongside potent Th1/Th17 responses, we therefore conclude that the vaccine induced a strong Th1-Th17 response with only modest Th2-Treg activity and this may have contributed to the protection observed.

The superior immunogenicity of Ag85B over ESAT-6 has also been observed in other studies where both antigens were used together (Dietrich et al., 2006;van Dissel et al., 2011), Ag85B is known to be one of the most immunogenic TB antigens whilst ESAT-6 is weakly immunogenic. Nevertheless both antigens have been previously shown to be protective, particularly when used in combination (Dietrich et al., 2006;van Dissel et al., 2011).

Ichihashi et al showed that PS could deliver antigens to APCs resulting in the stimulation of helper and cytotoxic T cell responses *in vivo* (Ichihashi et al., 2013). In keeping with those observations, a flow cytometry assay measuring Ki67 expression

indicated that the CD8 T cells from the Lipo-AE group proliferated robustly in response to Ag85B antigen and had a CD62L^{Low}/CD44^{High} phenotype.

CD4+ T cell responses to aerosol *Mtb* challenge are characterized by a delayed recruitment of effector T cells in the lungs, potentially hampering the host's response to infection and permitting the bacteria to establish a persistent infection (Reiley et al., 2008). The rationale behind the heterologous systemic prime mucosal boost strategy was to elicit a robust systemic response with a strong mucosal component to challenge the pathogen on entry. Recently, tissue-memory resident T (Trm) cells have become topical in the field. Thus, Perdomo et al demonstrated that mucosal but not subcutaneous, BCG immunisation generates lung resident memory T cell populations that mediate protection against TB (Perdomo et al., 2016). We established that Lipo-AE given mucosally could generate Trm, characterised as CD69+CD103+ memory T cells in the lung parenchyma. These cells were found to belong to both CD4 and CD8 compartment and are likely to be antigen specific, though we have no formal evidence of their antigen specificity as we did not have appropriate MHC tetramers to confirm this.

In conclusion, boosting BCG with Lipo-AE mediated enhanced immunity and protection over that afforded by BCG alone. This vaccine delivery platform is well suited for TB but the liposomal system can be adapted to suit other diseases and recently the first ever liposomes-adjuvanted vaccine was licensed indicated for malaria (Hawkes, 2015;Morrison, 2015), while a therapeutic vaccine candidate RUTI formulated in liposomes is currently in clinical trials (Cardona, 2006). This underscores the potential of liposome technology as an attractive vaccine delivery system.

Acknowledgement: This work was supported by the European Community H2020 grant No 643558.

Author contribution: G.R.D, A.C and P.H. performed all immunisation and Mtb infection experiments, as well as key immunological analyses. M-Y.K. performed bronchoalveolar antibody analysis; A.C.T. performed statistical analysis; N.P. generated Lipo-AE and performed APC experiments; M.J.P. contributed to processing of tissues and setting up CFUs; M.S. provided antigens; M.F. conceived the potential use of liposomes as a vaccine delivery platform. G.R.D., M.F. and R.R. co-wrote the manuscript.

Conflict of interest: The funders had no role in study design, data collection, and analysis, decision to publish, or preparation of the manuscript. Author Mahavir Singh was employed by company Lionex GmBH. All other authors declare no competing interests.

Figure legends

Fig. 1 Encapsulation and stability of PS/PS liposomes and their physical characteristics. The stability of PS liposomes carrying Alexafluor488-BSA was assessed for fluorescence intensity by flow cytometry and size distribution by Malverin Zetasizer, immediately and after 30 days from liposome generation and storage at 4°C.

(A) Schematic showing PS/PS liposome encapsulating an antigen

(B) Overlay of flow cytometry histogram plots of AF488-BSA loaded liposomes with 'empty' liposomes over time. Grey corresponds to empty liposomes while green corresponds to AF488-BSA liposomes after 30 days storage at 4^{o} C.

(C) Size distribution measured by Zetasizer of Ag85B-loaded liposomes following 30 day storage at 4 ^{o}C.

Fig. 2 Antigen internalization and processing in human DC after delivery by PS liposome**.**

(A) Immature and mature DC cells were exposed to dialyzed PS liposomes loaded with AF647-BSA to a ratio of 5:1 for 1 hour. Analysis was performed by flow cytometry.

(B) Immature DC cells were stained with the nucleic acid stain Hoechst and the acidophilic dye Lysotraker Red and stimulated with PS liposomes loaded withAF647-BSA at the ratio 5:1 for 90 minutes. A representative image from over many taken by confocal microscopy, is shown. Sample analysis indicated majority of cells positively stained with approximately 23 % strongly positive for both stains.

(C) Immature DC cells were exposed to PS liposomes loaded with DQ-OVA or to empty liposomes at a ratio of 5:1 for 1 hour. Red and green fluorescence was evaluated by flow cytometry. A representative experiment with cells from one, out of three, healthy donors is shown.

Fig. 3 Reduced *Mtb* infection in Lipo-AE immunised mice. Four weeks after the final immunisation, mice were challenged with aerosolised *Mtb* and then four weeks later culled and organs harvested for bacterial enumeration. Each point corresponds to log CFU value for the individual animals (n=7).

(A) Schematic depicting immunisation and Mtb infection schedule

(B) CFU in the lungs and spleens

The horizontal bars represent the mean for each group ± SEM. Log transformed data were analysed using a 1-way ANOVA and a Dunnett's multiple comparison test comparing all groups to the BCG control or comparing Lipo-AE with empty liposomes (Lipo); * P ≤ 0.05, ** P≤ 0.01, *** P ≤ 0.001, **** P ≤ 0.0001.

Fig. 4 Mucosal antibody responses and lung Trm induced by Lipo-AE.

(A) Levels of anti-Ag85B specific BAL IgG and IgA determined by antigen-specific ELISA. Each bar corresponds to the mean of triplicate samples from 3 animals from each group ± SEM. The set of bars represent 3-fold serial dilutions from the starting neat sample. Average end point titres are indicated above the bars.

(B) Analysis of the lung resident memory T cell populations**.** Except for the PBS group, animals were vaccinated with BCG sc and then with Lipo-AE or empty liposomes, both containing PolyIC, as described in Methods. Cells isolated from the lungs of immunised animals were stained and analysed by flow cytometry to determine the Trm populations. The gating strategy used was cells -> single cells -> live cells -> CD3+ -> CD4+/CD8+ -> CD44 ^{high} / CD62L^{low} and the CD69/CD103 double positive Trm presented. Data originated from n=3 pooled animals and a representative plot is shown.

.

Fig. 5 Cellular immune response induced by Lipo-AE.

(A) Antigen specific splenocyte and T cell proliferation. Splenocytes harvested from immunised animals were stimulated with Ag85B (blue) o ESAT-6 (red) as the recall antigens and media alone as the negative control, and proliferative

responses were then measured by radiolabelled thymidine incorporation. Vertical bars represent the stimulation indices (stimulation index = antigen specific radioactive counts per minute / background radioactive counts per minute).

(B) CD8 T cell proliferation. Splenocytes were stimulated with the recall antigens and the CD8+ Ki67+ cells identified. The gating strategy used was cells -> single cells -> live cells -> CD90.2+ -> CD8+ -> KI67+ and CD44/CD62L cells. The bars represent the percent of CD8+ cells that are Ki67+ and are broken down based on memory marker phenotype.

(C) **D, E** and **F**: Cytokine production following antigen recall assay. Splenocyte stimulation culture supernatants were collected and assayed for cytokine presence by. Legendplex: IFN-y (C), IL-10 (D), IL-17 (E) and IL-4 (F). Bars depict means pg/ml +/-SEM, with * indicating statistically significant values above the background ($P<0.05$).

Fig. 6 Polyfunctional T cell responses induced by Lipo-AE.

Splenocytes isolated from immunised animals were stimulated with Ag85B and the production of IFN-γ, IL-2, IL-17A and TNF-α measured by intracellular cytokine staining and flow cytometry.

(A) and (F) Proportion of CD4 and CD8 positive cells producing cytokines

(B) and (G) Proportion of CD4 and CD8 cells expressing each individual cytokine

(C) and (H) Proportion of CD4 abd CD8 cells producing at least 3 or 4 cytokines

(D) and (I) Polyfunctional CD4 and CD8 T cells phenotype by cytokine combinations

(E) and (J) Frequency of single or multiple cytokine producing CD4 and CD8 T cells as a proportion of all antigen specific cells

Gating strategy was the same as in our recent report (Hart et al., 2018).

Figure 7. Analysis of the lung resident memory T cell populations. Except for the PBS group, animals were vaccinated with BCG sc and then received one s.c. and one i.n. administration of Lipo-AE or empty PS/PS liposomes with PolyIC. Cells isolated from the lungs of immunised animals were stained and analysed by flow cytometry to determine the Trm populations. The gating strategy used was cells -> single cells -> live cells -> CD3+ -> CD4+/CD8+ -> CD44 ^{high} / CD62L^{low} and the CD69/CD103 double positive Trm presented. Data originated from n=3 pooled animals and a representative plot is shown.

References

Ambrosch, F., Wiedermann, G., Jonas, S., Althaus, B., Finkel, B., Gluck, R., and Herzog, C. (1997). Immunogenicity and protectivity of a new liposomal hepatitis A vaccine. *Vaccine* 15, 1209-1213.

Cardona, P.J. (2006). RUTI: a new chance to shorten the treatment of latent tuberculosis infection. Tuberculosis (Edinb) 86:273-289.

Childers, N.K., Michalek, S.M., Denys, F., and Mcghee, J.R. (1987). Characterization of liposomes for oral vaccines. *Adv Exp Med Biol* 216B, 1771-1780.

Churchyard, G., Kim, P., Shah, N.S., Rustomjee, R., Gandhi, N., Mathema, B., Dowdy, D., Kasmar, A., and Cardenas, V. (2017). What We Know About Tuberculosis Transmission: An Overview. *J Infect Dis* 216, S629-S635.

Dietrich, J., Andersen, C., Rappuoli, R., Doherty, T.M., Jensen, C.G., and Andersen, P. (2006). Mucosal administration of Ag85B-ESAT-6 protects against infection with Mycobacterium tuberculosis and boosts prior bacillus Calmette-Guerin immunity. *J Immunol* 177, 6353-6360.

Ellens, H., Morselt, H., and Scherphof, G. (1981). In vivo fate of large unilamellar sphingomyelin-cholesterol liposomes after intraperitoneal and intravenous injection into rats. *Biochim Biophys Acta* 674, 10-18.

Elson, C.O., Beagley, K.W., Sharmanov, A.T., Fujihashi, K., Kiyono, H., Tennyson, G.S., Cong, Y., Black, C.A., Ridwan, B.W., and Mcghee, J.R. (1996). Hapten-induced model of murine inflammatory bowel disease: mucosa immune responses and protection by tolerance. *J Immunol* 157, 2174-2185.

Fadok, V.A., Voelker, D.R., Campbell, P.A., Cohen, J.J., Bratton, D.L., and Henson, P.M. (1992). Exposure of phosphatidylserine on the surface of apoptotic lymphocytes triggers specific recognition and removal by macrophages. *J Immunol* 148, 2207-2216.

Flynn, J.L., Chan, J., Triebold, K.J., Dalton, D.K., Stewart, T.A., and Bloom, B.R. (1993). An essential role for interferon gamma in resistance to Mycobacterium tuberculosis infection. *J Exp Med* 178, 2249-2254.

Fortsch, D., Rollinghoff, M., and Stenger, S. (2000). IL-10 converts human dendritic cells into macrophage-like cells with increased antibacterial activity against virulent Mycobacterium tuberculosis. *J Immunol* 165, 978-987.

Fulton, S.A., Cross, J.V., Toossi, Z.T., and Boom, W.H. (1998). Regulation of interleukin-12 by interleukin-10, transforming growth factor-beta, tumor necrosis factor-alpha, and interferon-gamma in human monocytes infected with Mycobacterium tuberculosis H37Ra. *J Infect Dis* 178, 1105-1114.

Gallegos, A.M., Van Heijst, J.W., Samstein, M., Su, X., Pamer, E.G., and Glickman, M.S. (2011). A gamma interferon independent mechanism of CD4 T cell mediated control of M. tuberculosis infection in vivo. *PLoS Pathog* 7, e1002052.

Gideon, H.P., Phuah, J., Myers, A.J., Bryson, B.D., Rodgers, M.A., Coleman, M.T., Maiello, P., Rutledge, T., Marino, S., Fortune, S.M., Kirschner, D.E., Lin, P.L., and Flynn, J.L. (2015). Variability in tuberculosis granuloma T cell responses exists, but a balance of pro- and anti-inflammatory cytokines is associated with sterilization. *PLoS Pathog* 11, e1004603.

Greco, E., Quintiliani, G., Santucci, M.B., Serafino, A., Ciccaglione, A.R., Marcantonio, C., Papi, M., Maulucci, G., Delogu, G., Martino, A., Goletti, D., Sarmati, L., Andreoni, M., Altieri, A., Alma, M., Caccamo, N., Di Liberto, D., De Spirito, M., Savage, N.D., Nisini, R., Dieli, F., Ottenhoff, T.H., and Fraziano, M. (2012). Janus-faced liposomes enhance antimicrobial innate immune response in Mycobacterium tuberculosis infection. *Proc Natl Acad Sci U S A* 109, E1360-1368.

Gregoriadis, G. (1990). Immunological adjuvants: a role for liposomes. *Immunol Today* 11, 89-97.

Hart, P., Copland, A., Diogo, G.R., Harris, S., Spallek, R., Oehlmann, W., Singh, M., Basile, J., Rottenberg, M., Paul, M.J., and Reljic, R. (2018). Nanoparticle-Fusion Protein Complexes Protect against Mycobacterium tuberculosis Infection. *Mol Ther* 26, 822-833.

Hawkes, N. (2015). European Medicines Agency approves first malaria vaccine. *BMJ* 351, h4067.

Ichihashi, T., Satoh, T., Sugimoto, C., and Kajino, K. (2013). Emulsified phosphatidylserine, simple and effective peptide carrier for induction of potent epitope-specific T cell responses. *PLoS One* 8, e60068.

Jackson, S., Mestecky, J., Childers, N.K., and Michalek, S.M. (1990). Liposomes containing anti-idiotypic antibodies: an oral vaccine to induce protective

secretory immune responses specific for pathogens of mucosal surfaces. *Infect Immun* 58, 1932-1936.
Jankovic, D., and Trinchieri, G. (2007). IL-10 or not IL-10: that is the question. *Nat Immunol* 8, 1281-1283.
Khader, S.A., Bell, G.K., Pearl, J.E., Fountain, J.J., Rangel-Moreno, J., Cilley, G.E., Shen, F., Eaton, S.M., Gaffen, S.L., Swain, S.L., Locksley, R.M., Haynes, L., Randall, T.D., and Cooper, A.M. (2007). IL-23 and IL-17 in the establishment of protective pulmonary CD4+ T cell responses after vaccination and during Mycobacterium tuberculosis challenge. *Nat Immunol* 8, 369-377.
Kovacsovics-Bankowski, M., and Rock, K.L. (1995). A phagosome-to-cytosol pathway for exogenous antigens presented on MHC class I molecules. *Science* 267, 243-246.
Kwak, L.W., Pennington, R., Boni, L., Ochoa, A.C., Robb, R.J., and Popescu, M.C. (1998). Liposomal formulation of a self lymphoma antigen induces potent protective antitumor immunity. *J Immunol* 160, 3637-3641.
Lachman, L.B., Ozpolat, B., and Rao, X.M. (1996). Cytokine-containing liposomes as vaccine adjuvants. *Eur Cytokine Netw* 7, 693-698.
Michalek, S.M., Childers, N.K., Katz, J., Dertzbaugh, M., Zhang, S., Russell, M.W., Macrina, F.L., Jackson, S., and Mestecky, J. (1992). Liposomes and conjugate vaccines for antigen delivery and induction of mucosal immune responses. *Adv Exp Med Biol* 327, 191-198.
Mittrucker, H.W., Steinhoff, U., Kohler, A., Krause, M., Lazar, D., Mex, P., Miekley, D., and Kaufmann, S.H. (2007). Poor correlation between BCG vaccination-induced T cell responses and protection against tuberculosis. *Proc Natl Acad Sci U S A* 104, 12434-12439.
Miyanishi, M., Tada, K., Koike, M., Uchiyama, Y., Kitamura, T., and Nagata, S. (2007). Identification of Tim4 as a phosphatidylserine receptor. *Nature* 450, 435-439.
Morrison, C. (2015). Landmark green light for Mosquirix malaria vaccine. *Nat Biotechnol* 33, 1015-1016.
Nisini, R., Poerio, N., Mariotti, S., De Santis, F., and Fraziano, M. (2018). The Multirole of Liposomes in Therapy and Prevention of Infectious Diseases. *Front Immunol* 9, 155.
Ottenhoff, T.H., and Kaufmann, S.H. (2012). Vaccines against tuberculosis: where are we and where do we need to go? *PLoS Pathog* 8, e1002607.
Perdomo, C., Zedler, U., Kuhl, A.A., Lozza, L., Saikali, P., Sander, L.E., Vogelzang, A., Kaufmann, S.H., and Kupz, A. (2016). Mucosal BCG Vaccination Induces Protective Lung-Resident Memory T Cell Populations against Tuberculosis. *MBio* 7.
Redford, P.S., Murray, P.J., and O'garra, A. (2011). The role of IL-10 in immune regulation during M. tuberculosis infection. *Mucosal Immunol* 4, 261-270.
Reiley, W.W., Calayag, M.D., Wittmer, S.T., Huntington, J.L., Pearl, J.E., Fountain, J.J., Martino, C.A., Roberts, A.D., Cooper, A.M., Winslow, G.M., and Woodland, D.L. (2008). ESAT-6-specific CD4 T cell responses to aerosol Mycobacterium tuberculosis infection are initiated in the mediastinal lymph nodes. *Proc Natl Acad Sci U S A* 105, 10961-10966.
Reljic, R. (2007). IFN-gamma therapy of tuberculosis and related infections. *J Interferon Cytokine Res* 27, 353-364.
Rodrigues, L.C., Pereira, S.M., Cunha, S.S., Genser, B., Ichihara, M.Y., De Brito, S.C., Hijjar, M.A., Dourado, I., Cruz, A.A., Sant'anna, C., Bierrenbach, A.L., and Barreto, M.L. (2005). Effect of BCG revaccination on incidence of tuberculosis

in school-aged children in Brazil: the BCG-REVAC cluster-randomised trial. *Lancet* 366, 1290-1295.
Romero, E.L., and Morilla, M.J. (2011). Topical and mucosal liposomes for vaccine delivery. *Wiley Interdiscip Rev Nanomed Nanobiotechnol* 3, 356-375.
Roth, A.E., Benn, C.S., Ravn, H., Rodrigues, A., Lisse, I.M., Yazdanbakhsh, M., Whittle, H., and Aaby, P. (2010). Effect of revaccination with BCG in early childhood on mortality: randomised trial in Guinea-Bissau. *BMJ* 340, c671.
Sakai, S., Kauffman, K.D., Sallin, M.A., Sharpe, A.H., Young, H.A., Ganusov, V.V., and Barber, D.L. (2016). CD4 T Cell-Derived IFN-gamma Plays a Minimal Role in Control of Pulmonary Mycobacterium tuberculosis Infection and Must Be Actively Repressed by PD-1 to Prevent Lethal Disease. *PLoS Pathog* 12, e1005667.
Schlegel, R.A., and Williamson, P. (2001). Phosphatidylserine, a death knell. *Cell Death Differ* 8, 551-563.
Sigal, L.J., Crotty, S., Andino, R., and Rock, K.L. (1999). Cytotoxic T-cell immunity to virus-infected non-haematopoietic cells requires presentation of exogenous antigen. *Nature* 398, 77-80.
Tanaka, Y., and Schroit, A.J. (1983). Insertion of fluorescent phosphatidylserine into the plasma membrane of red blood cells. Recognition by autologous macrophages. *J Biol Chem* 258, 11335-11343.
Van Dissel, J.T., Soonawala, D., Joosten, S.A., Prins, C., Arend, S.M., Bang, P., Tingskov, P.N., Lingnau, K., Nouta, J., Hoff, S.T., Rosenkrands, I., Kromann, I., Ottenhoff, T.H., Doherty, T.M., and Andersen, P. (2011). Ag85B-ESAT-6 adjuvanted with IC31(R) promotes strong and long-lived Mycobacterium tuberculosis specific T cell responses in volunteers with previous BCG vaccination or tuberculosis infection. *Vaccine* 29, 2100-2109.
Wassef, N.M., Alving, C.R., and Richards, R.L. (1994). Liposomes as carriers for vaccines. *Immunomethods* 4, 217-222.
Wigginton, J.E., and Kirschner, D. (2001). A model to predict cell-mediated immune regulatory mechanisms during human infection with Mycobacterium tuberculosis. *J Immunol* 166, 1951-1967.

Figure 1

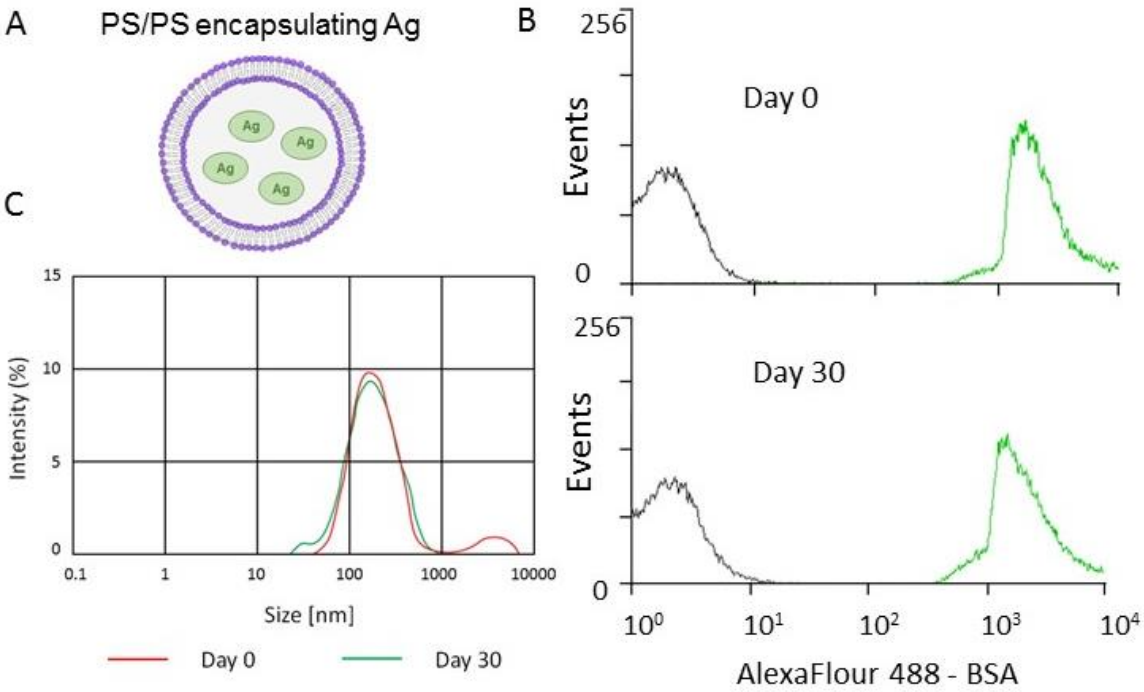
A
PS/PS encapsulating Ag
Ag
Ag
Ag
Ag
B
256
Day 0
Events
0
256
Day 30
Events
0
10^0
10^1
10^2
10^3
10^4
AlexaFlour 488 - BSA
C
15
10
5
0
Intensity (%)
0.1
1
10
100
1000
10000
Size [nm]
Day 0
Day 30

Figure 2

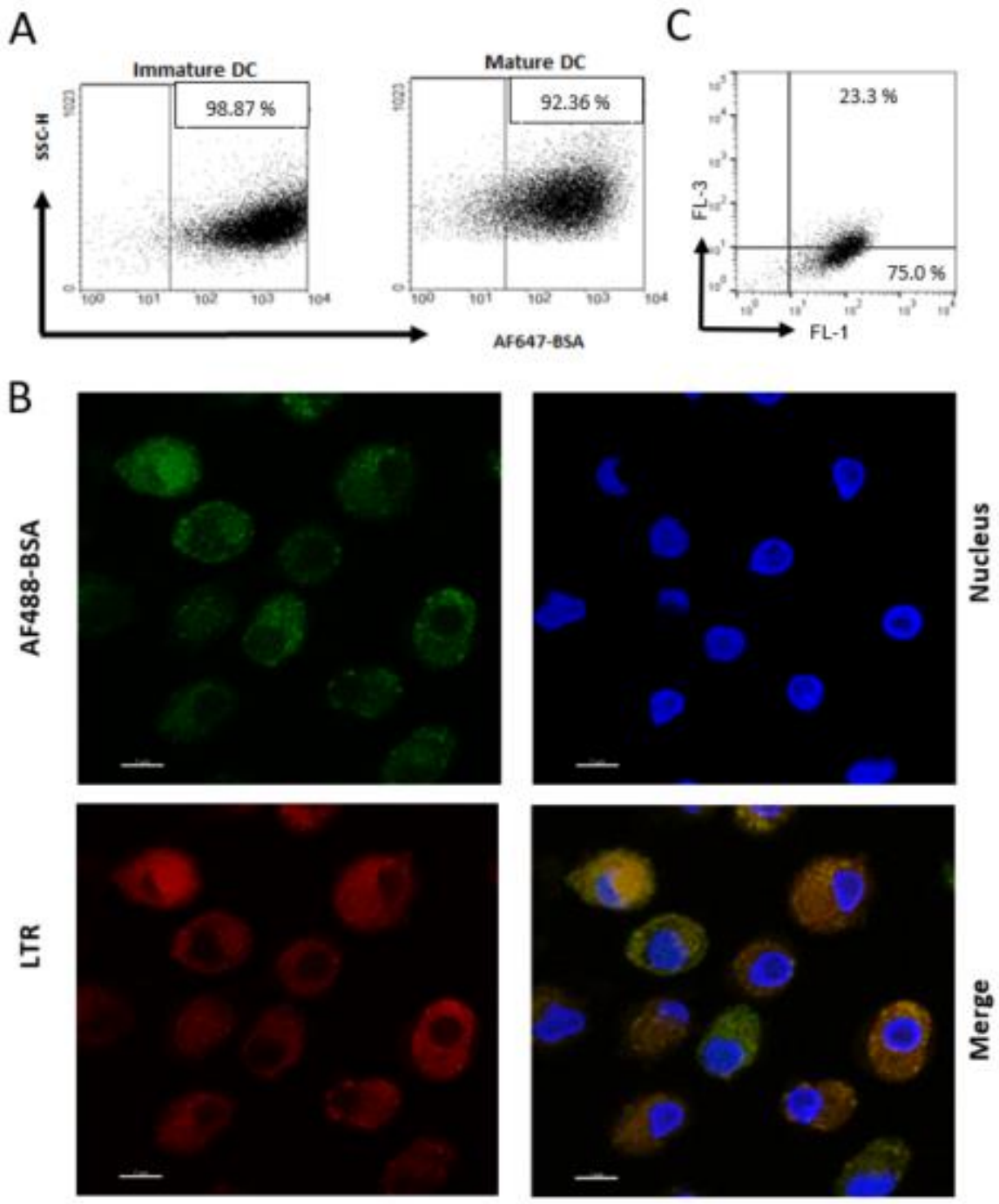
A
Immature DC
98.87 %
SSC-H
AF647-BSA
Mature DC
92.36 %
C
23.3 %
75.0 %
FL-3
FL-1
B
AF488-BSA
Nucleus
LTR
Merge

Figure 3

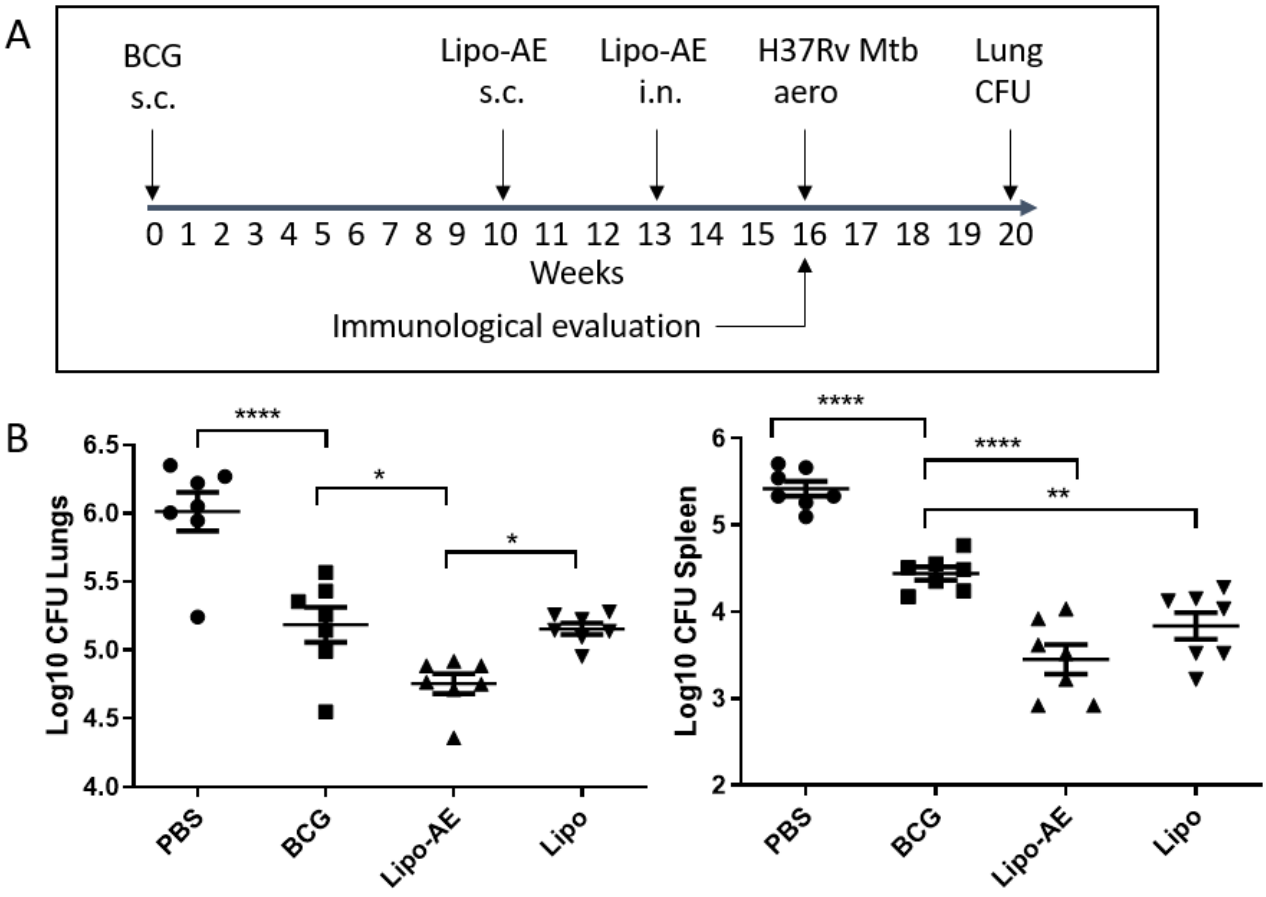
A
BCG
s.c.
Lipo-AE
s.c.
Lipo-AE
i.n.
H37Rv Mtb
aero
Lung
CFU
0 1 2 3 4 5 6 7 8 9 10 11 12 13 14 15 16 17 18 19 20
Weeks
Immunological evaluation
B
Log10 CFU Lungs
6.5
6.0
5.5
5.0
4.5
4.0
****
*
*
PBS
BCG
Lipo-AE
Lipo
Log10 CFU Spleen
6
5
4
3
2
****
****
**
PBS
BCG
Lipo-AE
Lipo

Figure 4

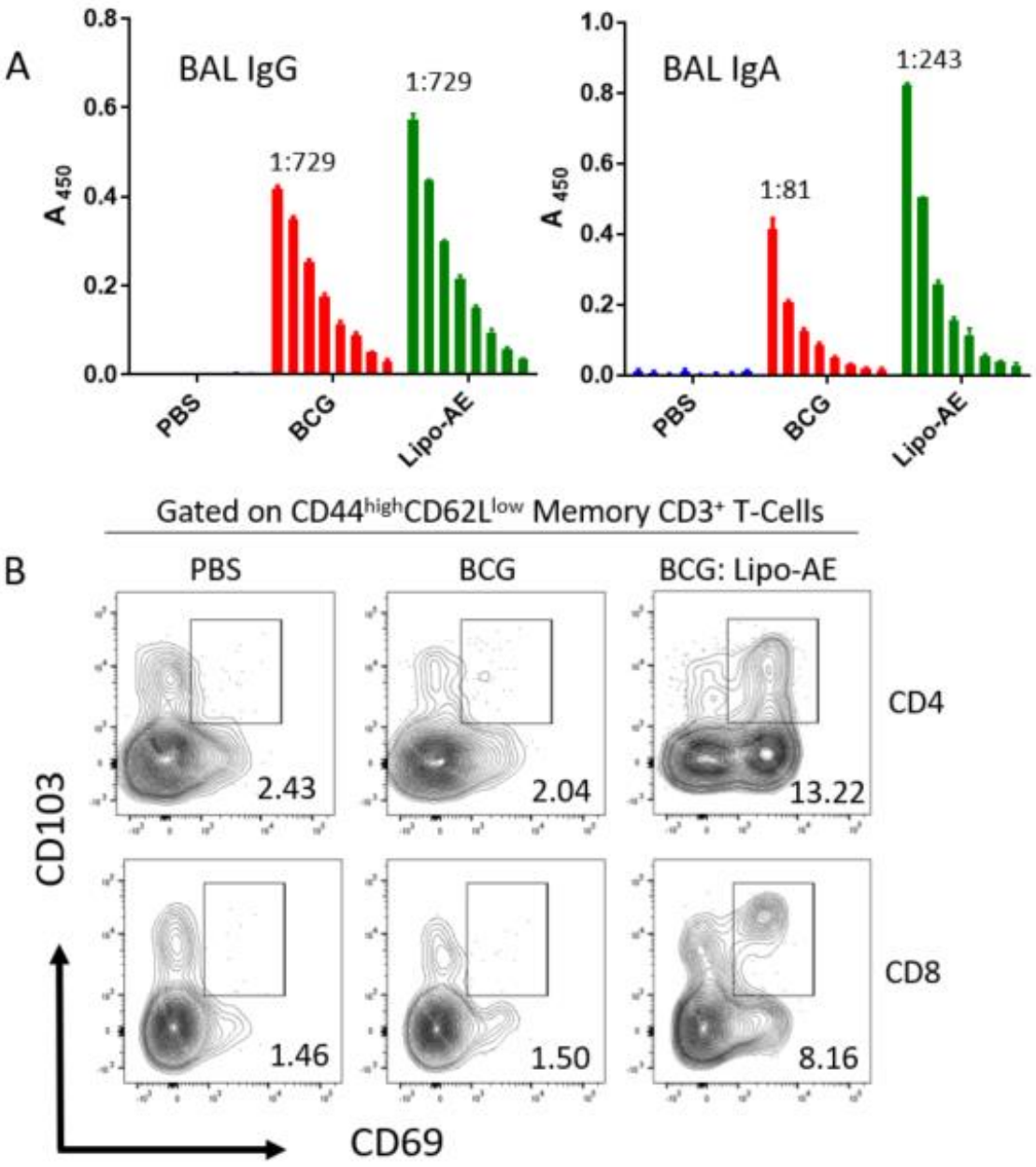
A
BAL IgG
1:729
1:729
A 450
0.8
0.6
0.4
0.2
0.0
PBS
BCG
Lipo-AE
BAL IgA
1:243
1:81
1.0
0.8
0.6
0.4
0.2
0.0
PBS
BCG
Lipo-AE
Gated on CD44highCD62Llow Memory CD3+ T-Cells
B
PBS
BCG
BCG: Lipo-AE
CD4
CD8
CD103
CD69
2.43
2.04
13.22
1.46
1.50
8.16

Figure 5

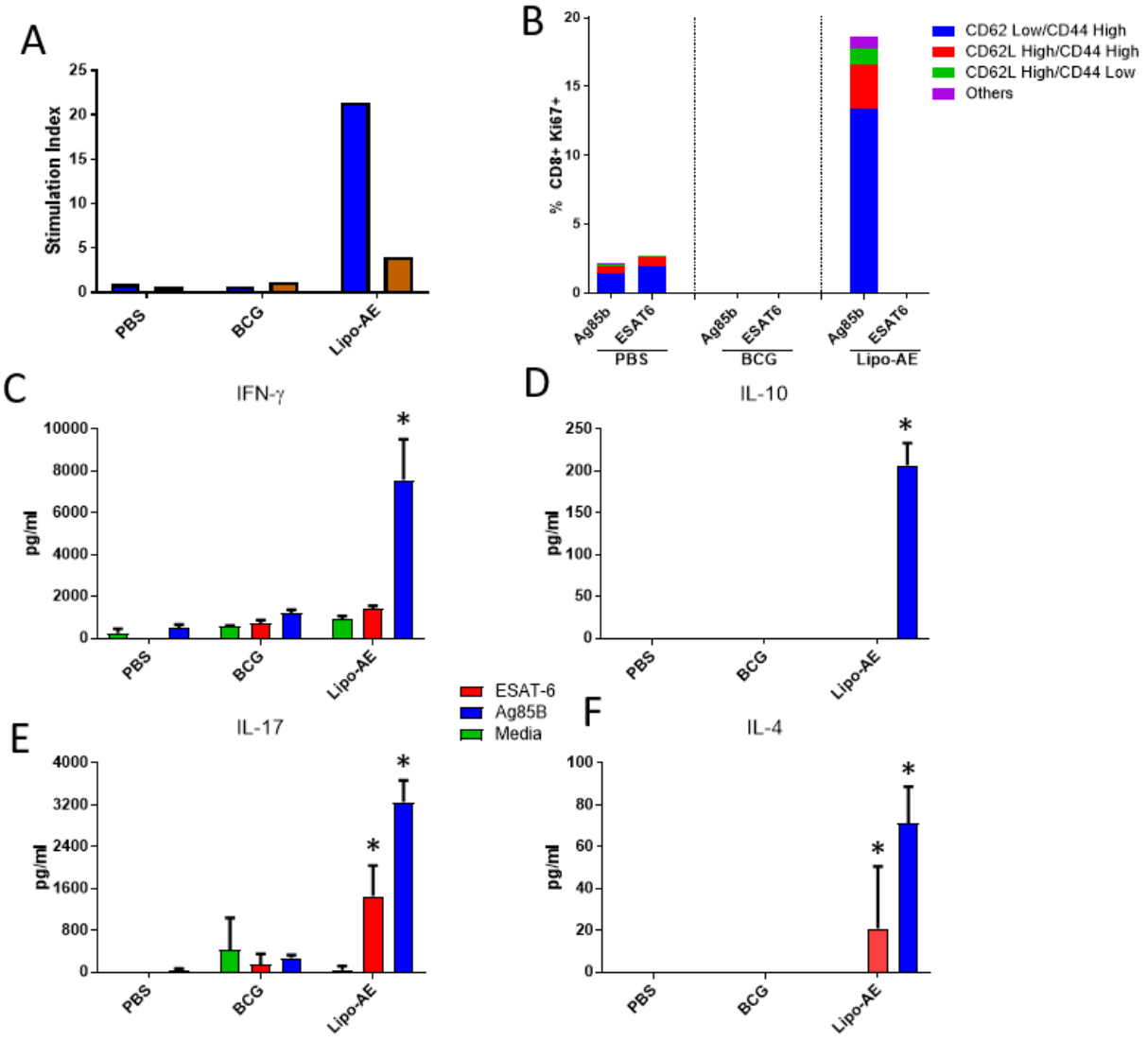
A
Stimulation Index
PBS
BCG
Lipo-AE
B
% CD8+ Ki67+
CD62 Low/CD44 High
CD62L High/CD44 High
CD62L High/CD44 Low
Others
Ag85b
ESAT6
PBS
BCG
Lipo-AE
C
IFN-γ
pg/ml
D
IL-10
pg/ml
ESAT-6
Ag85B
Media
E
IL-17
pg/ml
F
IL-4
pg/ml

Figure 6

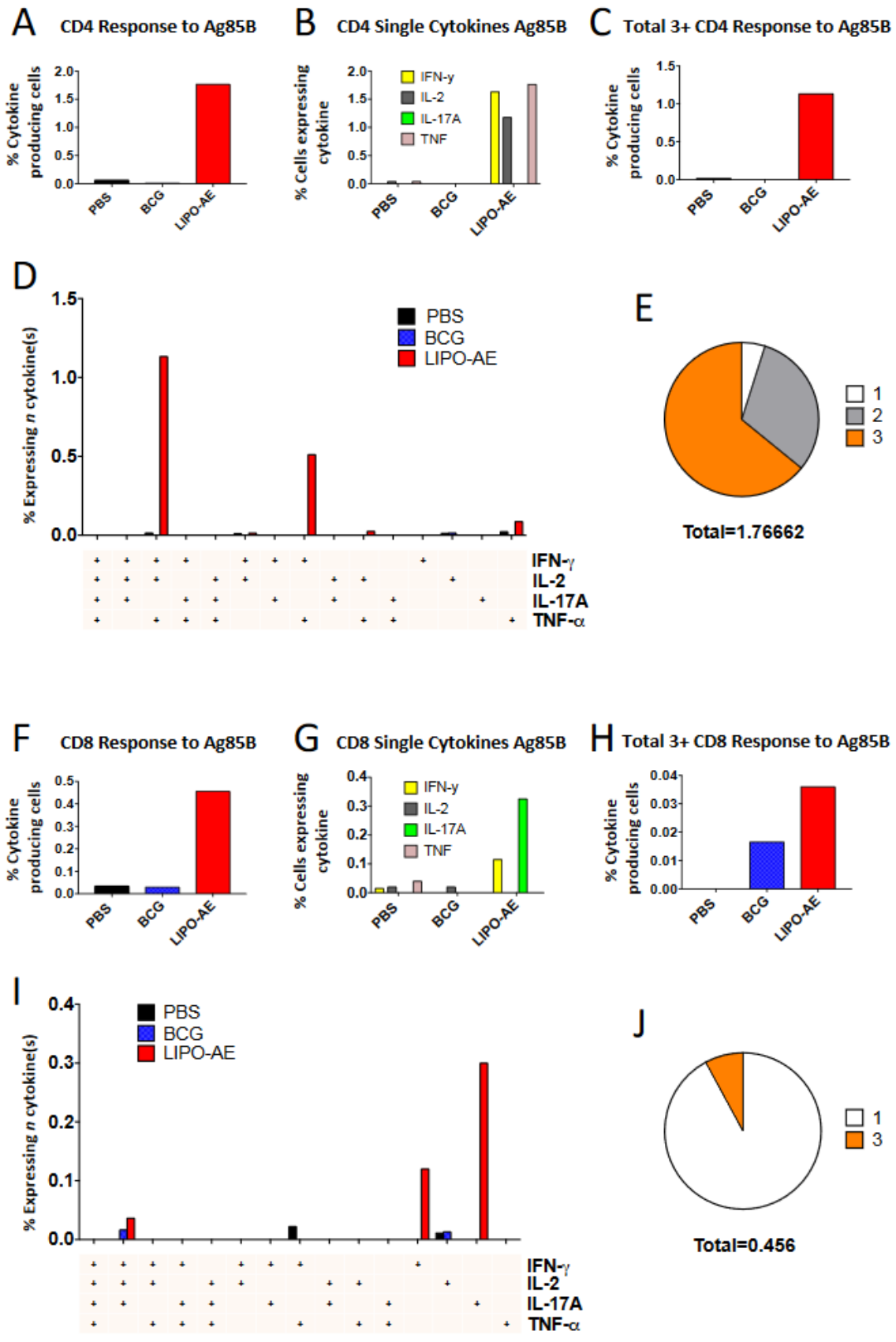
A
CD4 Response to Ag85B
% Cytokine producing cells
PBS
BCG
LIPO-AE
B
CD4 Single Cytokines Ag85B
% Cells expressing cytokine
IFN-γ
IL-2
IL-17A
TNF
C
Total 3+ CD4 Response to Ag85B
D
% Expressing n cytokine(s)
E
1
2
3
Total=1.76662
IFN-γ
IL-2
IL-17A
TNF-α
F
CD8 Response to Ag85B
G
CD8 Single Cytokines Ag85B
H
Total 3+ CD8 Response to Ag85B
I
J
Total=0.456

Figure 7

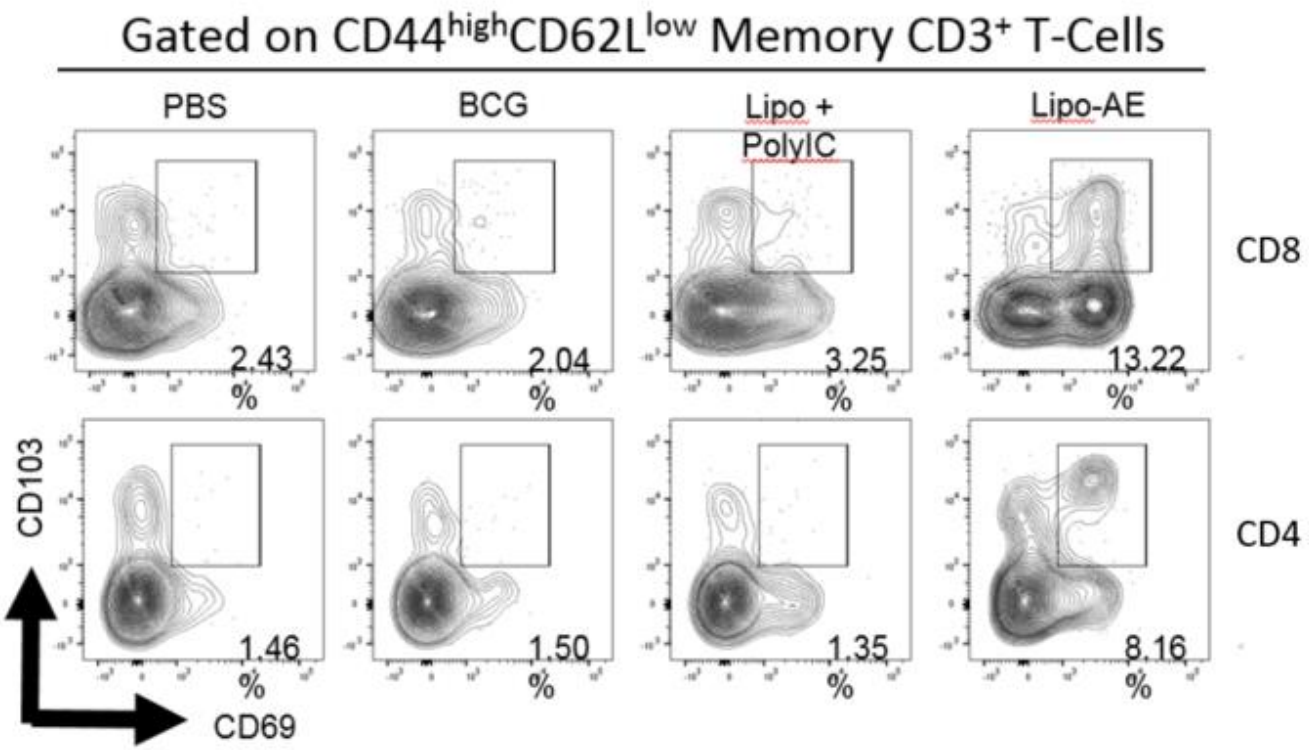
Gated on CD44highCD62Llow Memory CD3+ T-Cells
PBS
BCG
Lipo + PolyIC
Lipo-AE
CD8
CD4
CD103
CD69
2.43 %
2.04 %
3.25 %
13.22 %
1.46 %
1.50 %
1.35 %
8.16 %